Supporting Information

Samonds et al. 10.1073/pnas.1200125109

SI Text

Mean Firing Rate Statistics for Experimental Stimuli. We examined the impact of response changes caused by relative luminance for our population of disparity-tuned neurons in more detail. The examples in Fig. 2 suggest that the disk stimuli, and therefore relative luminance, have less influence on primary visual cortex (V1) responses compared with dynamic random dot stereograms (DRDSs) and therefore might not have sufficient impact for inferring disparity from the neuronal population. Fig. S1*A* shows the population histogram for the maximum mean firing rate measured for each stimulus and reveals that the neurons responded more strongly to DRDS [median = 35 spikes per second (sps)] compared with disks (median = 16 sps; Wilcoxon's rank sum test, $P < 1 \times 10^{-12}$), and the maximum mean firing rates were significantly correlated between the stimuli (Fig. S1*B*; Spearman's $\rho = 0.68$, $P < 1 \times 10^{-28}$). However, neurons respond strongly to DRDS stimuli not solely because of their disparity; a large portion of their response is caused by the spatiotemporal dynamics and strong localized contrast of the DRDS. If we compare the variability of the responses to the conditions that we tested for DRDSs and disks, the responsiveness to these two types of stimuli are more comparable (Fig. S1*C*), although the maximum change in mean firing rate is still significantly stronger for DRDSs (median = 12 sps) compared with disks (median = 11 sps; $P < 0.01$). These maximum changes in mean firing rate were also significantly correlated between the stimuli (Fig. S1*D*; $\rho = 0.53$, $P < 1 \times 10^{-15}$). Overall, these results suggest that changes in relative luminance could affect V1 responses nearly as much as disparity. Fig. 2 also supports that relative luminance and the changes in firing rates between the white and black disks, especially for near and far disparity-tuned neurons, appear to be strong enough that relative luminance should impact disparity-tuned neurons as much as considerable changes in disparity. For example, the difference between the responses to the white and black disks for the example neuron in Fig. 2*C* is equal to 64% of the maximum response difference for the disparity tuning curve for that same neuron shown in Fig. 2*D*, which would be caused by a >0.30° difference from the preferred disparity. And the difference between the responses to the white and black disks for the example neuron in Fig. 2*E* is equal to 36% of the maximum response difference for the disparity tuning curve for that same neuron shown in Fig. 2*F*, which would be caused by a >0.20° difference from the preferred disparity.

Stability of Luminance Index with Varying Disk Size. We tested the robustness of the relative luminance responses by examining the variation in the luminance index across a wider range of disk sizes. For a separate population of 97 neurons recorded in monkey I, we computed the luminance index for responses to white and black disks with diameters of 3°, 5°, 7°, 9°, 12°, and 15°. The mean luminance index varied little with diameter (Fig. S3*A*). To illustrate that this low variation was consistent across the entire range of luminance index values and diameter sizes, we plotted the luminance index value computed for the response of each neuron to one diameter vs. the result computed from the response to another diameter. With six diameters, there are 15 possible pairs of diameters to compare. In Fig. S3*B*, we show the data points for all 15 pairs plotted simultaneously ($n = 15$ pairs × 97 neurons = 1,455 data points), and in Fig. S3*C*, we show the individual scatter plot for each possible diameter comparison ($r > 0.57$, $P < 1 \times 10^{-10}$ for all scatter plots). For a small subset of these neurons ($n = 23$), we also measured the preferred binocular disparity using the DRDS so that we could show that the low variation in luminance index also translated into low variation in our correlation estimate (Fig. S3*D*). Although the sample size was too small to exhibit significance for all diameters, the correlation estimated was always < –0.20.

Stability of Preferred Binocular Disparity with Varying Spatial Scale. We tested the robustness of our preferred disparity estimates by varying spatial characteristic of DRDSs. For a population of n = 81 neurons that partially overlapped with the data described in the main text, we measured disparity tuning from the responses to the DRDS with three different aperture sizes (Fig. S4*A*; 2°, 3°, and 4°). Although disparity tuning curves for larger stimuli were sharper, the location of the peak, or the preferred disparity, varied very little between the three conditions. Fig. S4*C* illustrates this result by showing that the preferred disparity was highly correlated between any of the comparisons between aperture sizes ($r > 0.90$, $P < 10^{-29}$). A subset of this population ($n = 22$ neurons) overlapped with the data described in the main text so we could also test how the correlation between preferred disparity and luminance index varied with aperture size. Fig. S4*D* shows that the correlation changed very little with changes in aperture size ($r < -0.36$, $P < 0.1$).

For a separate population of 22 neurons recorded in monkey I, we also measured disparity tuning with the DRDS with three different dot sizes (Fig. S4*B*; 0.1°, 0.2°, and 0.3°). Similar to the aperture experiment, the shape of the tuning curve varied between dot sizes, but there were not large changes in the location of the peak. The preferred disparities estimated from DRDS stimuli with different dot sizes were highly correlated for all possible comparisons (Fig. S4*E*, $r > 0.63$, $P < 0.002$).

Stability of Correlation with Alternative Luminance Index Mathematical Definitions. We chose the simplest ratio to describe the response of light disks relative to dark disks, which is the ratio of the mean firing rate to the 50% contrast white disk (W) compared with the 50% contrast black disk (B):

$$\text{Luminance index} = \frac{W - B}{W + B}. \qquad \textbf{[S1]}$$

However, we did test several different metrics including a ratio that corrected for baseline mean firing rate (to a mean luminance gray screen or 0% contrast, G),

$$\text{LI}_{\text{baseline}} = \frac{(W - G) - (B - G)}{|W - G| + |B - G|}; \qquad \textbf{[S2]}$$

a ratio that used the mean firing rates for all of the disks (all contrasts n) that were presented or the area under the contrast response curves for light (w) and dark (b) disks (Fig. 2 *C* and *E*),

$$\text{LI}_{\text{area}} = \frac{\sum_{n=1}^{W} w_n - \sum_{n=1}^{B} b_n}{\sum_{n=1}^{W} w_n + \sum_{n=1}^{B} b_n}; \qquad \textbf{[S3]}$$

the center-of-mass, or the average contrast weighted by response strength, for the combined light and dark contrast response curves where c is the contrast, lighter-than-gray contrast is positive, darker-than-gray contrast is negative, and x is the mean firing rate,

$$\mathrm{LI}_{\mathrm{CoM}} = \frac{\sum_{n=B}^{W} c_n * x_n}{\sum_{n=B}^{W} x_n}; \qquad \textbf{[S4]}$$

and finally, a logarithmic ratio

$$\mathrm{LI}_{\log} = \log\left(\frac{W/G}{B/G}\right). \qquad \textbf{[S5]}$$

All five of the metrics for a luminance index resulted in a significant negative correlation with preferred binocular disparity with an absolute magnitude >0.2 ($n = 199$ neurons, $r < -0.20$, $P < 0.005$).

Range Database Considerations. There are relationships between brightness and distance in natural scenes other than those described in the main text that we considered. The intervening atmosphere can have several effects (collectively known as aerial perspective) on the brightness of distant objects. The first is the scattering of light, which makes distant objects appear more blurry. In outdoor daylight conditions, the atmosphere also acts to scatter light originating from the sky and deflect it toward the observer. This scattered light is known as "skylight". The greater the distance is between observer and object, the greater the amount of skylight that occurs in the intervening distance, making more distant objects brighter. Under sufficiently foggy conditions, this effect is even strong enough to estimate the relative locations of buildings in a city skyline (1). Although under normal conditions, most atmospheric particles (such as water vapor) primarily scatter light, another possible effect of the atmosphere is that larger opaque airborne particles, such as in smoke, may absorb light. This effect could make more distant objects appear darker. Both atmospheric effects are evident only over long distances in normal weather conditions. Because all of our range and image data were collected under sunny, clear conditions with a range limitation of ~300 m, the effects are unlikely to be present in our data. When these effects occur over long distances, they are unlikely to play a substantial role in stereoscopic vision and therefore influence disparity-tuned neurons in the visual cortex. Because these effects otherwise occur in foggy or smoky conditions, they are too infrequent to have a sufficient ecological impact in shaping the statistical trends stored within the human or nonhuman primate visual system.

Because our range sensor relies on echoes from laser pulses, no data were available from sky regions so pixels for the sky are not included in our analysis. However, most animals spend very little time foveating on the sky and tend to look downward much of the time (2). Nonetheless, we recomputed the results of Fig. 1 while including pairs such that one pixel was in the sky. All pixels that did not receive a laser echo were set at a distance of 11,000 m. There is still a strong negative correlation between disparity and relative intensity (Fig. S5*A*), and the probability that the nearer pixel is brighter was reduced minimally (Fig. S5*B*).

Stability of Correlation over Time. We examined how the correlation between luminance index and preferred binocular disparity evolved over time. We found that the smallest window of analysis that provided us stable estimates of luminance index and preferred disparity was 250 ms. We computed the mean firing rate for DRDS and white and black disk stimuli in sliding 250-ms windows every 1 ms over the stimuli duration. The mean firing rates for both DRDS and disk stimuli increased rapidly soon after stimulus onset and then slowly decreased over the stimulation period (Fig. S6*A*). The difference between the responses to white and black disks, as well as the location of the preferred disparity, was relatively stable over time. The negative correlation between these measurements was apparent when the mean firing rates increased after stimulus onset and remained stable and significant throughout stimulation, starting from the peak of the mean firing rates soon after response onset (Fig. S6*B*).

1. Narasimhan SG, Nayar SK (2002) Vision and the atmosphere. *Int J Comput Vis* 48: 233–254.

2. Liu Y, Bovik AC, Cormack LK (2008) Disparity statistics in natural scenes. *J Vis* 8: 19.1–19.14.

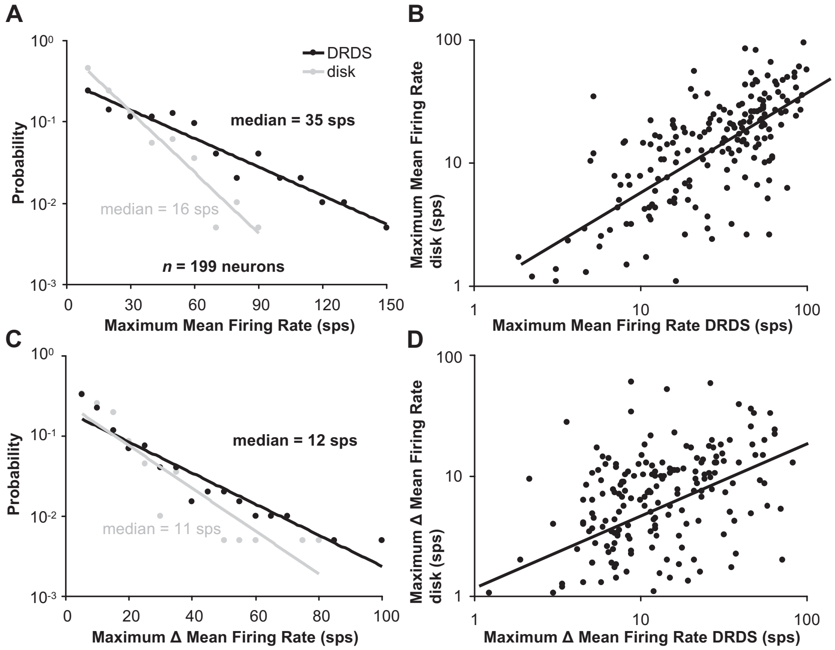

Fig. S1. The responsiveness to changes in relative luminance is comparable to that to changes in binocular disparity. (*A*) Histogram of maximum mean firing rates measured for neurons during disk and DRDS stimulation (*n* = 199 neurons). (*B*) Scatter plot of maximum mean firing rates measured for neurons during disk and DRDS stimulation. (*C*) Histogram of maximum change in mean firing rates measured for neurons during disk and DRDS stimulation. (*D*) Scatter plot of maximum change in mean firing rates measured for neurons during disk and DRDS stimulation.

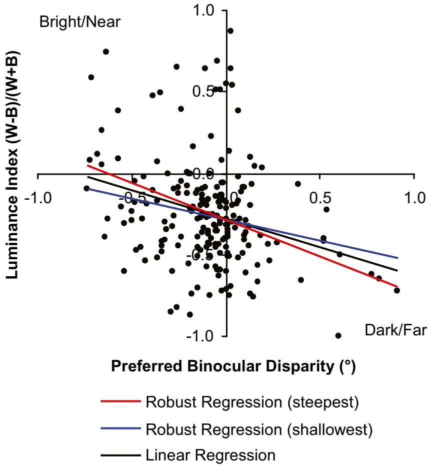

Fig. S2. Comparison of robust and linear regression analysis. The most extreme results are shown on the basis of a wide range of weighting functions and tuning constants.

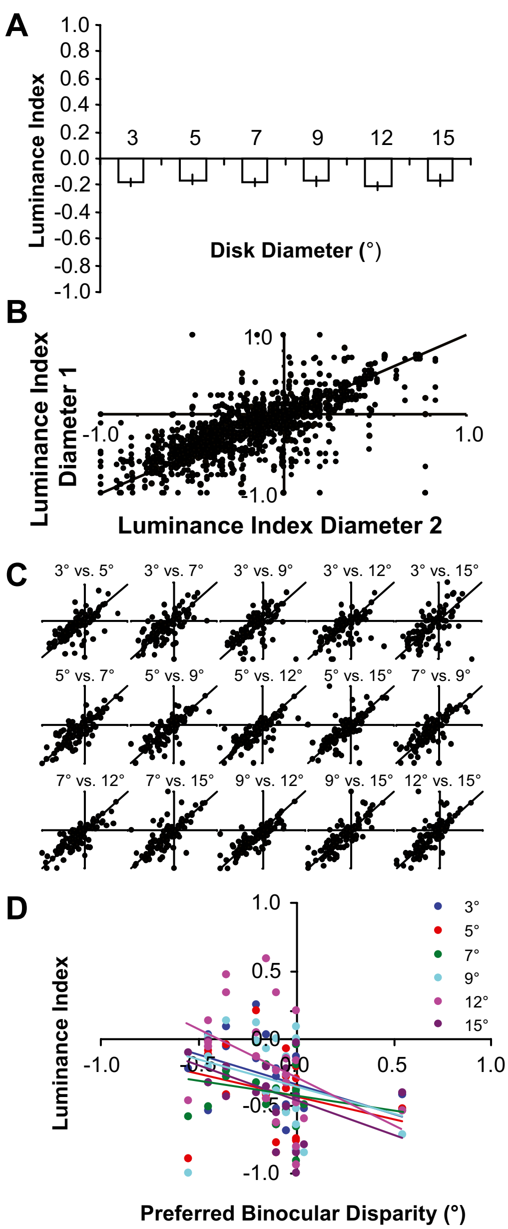

Fig. S3. Stability of luminance index with varying disk size. (*A*) Mean luminance index for disks with six different diameters (error bars are population SE, *n* = 97 neurons). (*B*) Aggregate scatter plot of luminance index computations for all 15 possible pairs of diameter comparisons. (*C*) Individual scatter plot of luminance index computations for all 15 possible pairs of diameter comparisons. (*D*) Scatter plot of luminance index vs. preferred binocular disparity for responses to all six diameters (*n* = 23 neurons).

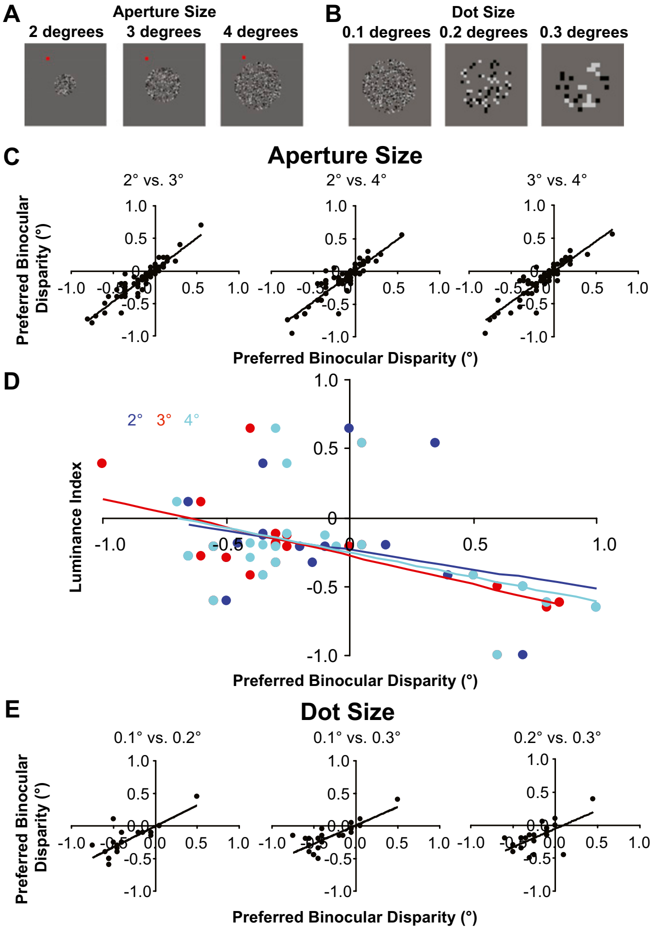

Fig. S4. Stability of preferred binocular disparity with varying spatial scale. (*A*) DRDS stimuli with varying aperture sizes used to measure binocular disparity tuning (image for one eye shown). (*B*) DRDS stimuli with varying dot sizes used to measure binocular disparity tuning. (*C*) Individual scatter plot of preferred binocular disparity for all three possible pairs of aperture diameter comparisons (*n* = 81 neurons). (*D*) Scatter plot of luminance index vs. preferred binocular disparity for all three aperture sizes (*n* = 22 neurons). (*E*) Individual scatter plot of preferred binocular disparity for all three possible pairs of dot size comparisons (*n* = 22 neurons).

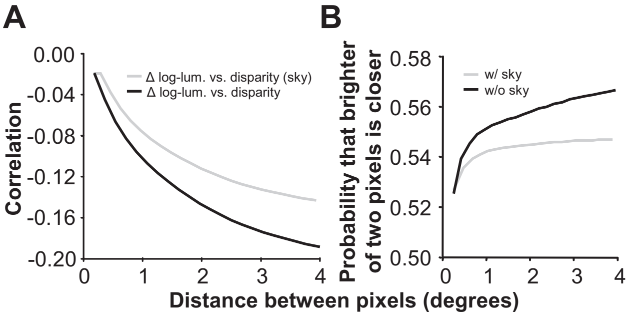

Fig. S5. Natural scene statistics when including image pixels from the sky. (*A*) Correlation between relative luminance and relative depth. (*B*) Given two pixels, the one that is lighter is more likely to be nearer.

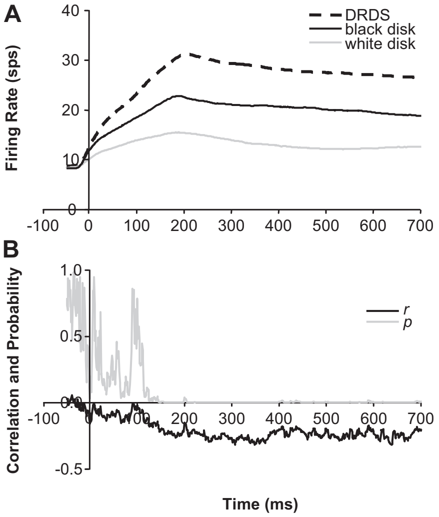

Fig. S6. Temporal dynamics of neuronal responses and correlation between relative luminance and preferred binocular disparity (*r*). All values were computed in 250-ms sliding windows every 1 ms. (*A*) Average mean firing rate of *n* = 199 neurons in response to DRDS and disk stimulation. (*B*) Correlation between luminance index and preferred disparity, *r*, and the significance of that correlation, *p*.